Effects of Breit interaction on the $L_{2,3}$ x-ray absorption near-edge structures of 3*d* transition metals

Hidekazu Ikeno* and Isao Tanaka
Department of Materials Science and Engineering, Kyoto University, Yoshida, Sakyo, Kyoto 606-8501, Japan
(Received 27 September 2007; published 27 February 2008)

$L_{2,3}$ x-ray absorption near-edge structures (XANES) of 3*d* transition metal (TM) ions and their compounds are calculated by the all-electron relativistic configuration interaction method. The Breit interaction term, which is the first relativistic correction term for the electron-electron interaction in the quantum electrodynamics, is taken into account in the many-electron Hamiltonian. Then the effects on the multiplet structure for 3*d* TM $L_{2,3}$ XANES are investigated. The energy separation between L_3 and L_2 edges of theoretical spectrum decreases when the Breit interaction term is taken into account. At the final states of $L_{2,3}$ XANES, the Breit interaction energies linearly depend on the occupation number of TM $2p_{3/2}$ orbitals. They are not influenced by the valency and the crystal field. This main contribution of the Breit interaction term is, therefore, calculated to be the reduction of the separation between L_3 and L_2 edges, which ranges from 0.49 to 1.52 eV for Sc to Cu.

DOI: 10.1103/PhysRevB.77.075127 PACS number(s): 78.70.Dm, 78.20.Bh, 71.15.Rf

I. INTRODUCTION

X-ray absorption near-edge structures (XANES) have been widely used to characterize the local environment of selected elements.[1–5] Since $L_{2,3}$ XANES measures the electric dipole transition from $2p_{1/2}$ and $2p_{3/2}$ orbitals to unoccupied *d* bands, it is useful for characterization of the oxidation and spin states of transition metal compounds. Recently, the present authors' group developed the hybrid method of density functional theory and configuration interaction method (DFT-CI) and applied it to the calculations of 3*d* transition metal (TM) $L_{2,3}$ XANES.[6–8] A relativistic molecular orbital (MO) calculation is made using model clusters with density functional theory. Electronic correlations among 3*d* electrons and a 2*p* hole were rigorously calculated by taking the Slater determinants made by the DFT-MOs mainly composed of TM 2*p* and TM 3*d* orbitals. Experimental spectra from many compounds having different *d*-electron numbers and coordination numbers have been successfully reproduced without any empirical parameters. The agreement between experimental and theoretical spectra is better when the dimension of Slater determinants is increased to include ligand *p* orbitals. Then, the electronic correlations among ligand *p*, TM 3*d* electrons, and 2*p* core-hole can be explicitly calculated.[8]

Despite the success in reproduction of experimental XANES by the calculation, small but non-negligible overestimation of the energy separation between L_3 and L_2 edges has been recognized in theoretical spectra calculated by the DFT-CI method. In these calculations, the spin-orbit coupling on core 2*p* level is automatically taken into account by solving the Dirac equation. The overestimation could be ascribed to improper treatment of the electron-electron interactions in the relativistic many-electron systems.

The motion of electrons should be described by the quantum electrodynamics (QED) in relativistic many-electron system, where the electrons do not interact directly with each other but through the electromagnetic field. In QED, the relativistic correction terms of the electron-electron interaction are given as a perturbation series of fine structure constant, α ($=c^{-1}$ in a.u.). The first correction term for the Coulomb interaction is called the Breit interaction term. When it is included into the electron-electron interaction operator, the Hamiltonian is called Dirac-Coulomb-Breit Hamiltonian, which is most commonly used in the relativistic many-electron atomic theory.

The contribution of the Breit interaction term has been theoretically examined for isolated atoms or ions.[9–19] Accuracy of transition energies such as $K\alpha$ x-ray emission energy, $K\beta$ hypersatellite energy, and intrashell excitation energy was reported to be improved when the Breit interaction term was taken into account. However, all of these calculations were made for isolated atoms or ions. No information is available for the dependence of the correction term on chemical states, such as oxidation number and crystal field.

In the present study, we include the Breit term in the electron-electron interaction operators of our all-electron CI calculations in order to examine the effects of the correction term on the $L_{2,3}$ XANES. Calculations were made not only for isolated 3*d* TM ions, but also for model clusters of oxide crystals. The influence of the Breit term on the multiplet structures corresponding to the 3*d* TM $L_{2,3}$ XANES and the separation between L_3 and L_2 edges are discussed in detail.

II. METHODS

The relativistic CI method used in the present work is the same as used in previous works,[6–8] except for the difference in the many-electron Hamiltonian. The effective many-electron Hamiltonian employed here is called "no-pair" Dirac-Coulomb or Dirac-Coulomb-Breit Hamiltonian,[20,21] described as

$$H^+ = \sum_{i=1}^{N} \Lambda_i^+ h_D(\boldsymbol{r}_i) \Lambda_i^+ + \sum_{i=1}^{N} \sum_{j<i} \Lambda_i^+ \Lambda_j^+ V_{\mathrm{ee}}(\boldsymbol{r}_i, \boldsymbol{r}_j) \Lambda_j^+ \Lambda_i^+ - \sum_{i=1}^{N} \Lambda_i^+ U_{\mathrm{eff}}(\boldsymbol{r}_i) \Lambda_i^+, \quad (1)$$

where N is the number of electrons in the model. h_D is the one-particle Dirac Hamiltonian given as

$$h_D(\boldsymbol{r}) = c\boldsymbol{\alpha}\cdot\boldsymbol{p} + c^2\beta + v_{\mathrm{nuc}}(\boldsymbol{r}) + v_{\mathrm{ext}}(\boldsymbol{r}) + U_{\mathrm{eff}}(\boldsymbol{r}) \quad (2)$$

in atomic units (a.u.), where $\boldsymbol{\alpha}$ and β are 4×4 Dirac matrices, c is the velocity of light, $v_{\mathrm{nuc}}(\boldsymbol{r})$ is the electrostatic potential from nuclei, and $v_{\mathrm{ext}}(\boldsymbol{r})$ is the external potential such as the Madelung potential. $U_{\mathrm{eff}}(\boldsymbol{r})$ is the effective potential of electron-electron interactions used for the MO calculation, which is subtracted from the many-electron Hamiltonian, H^+. Λ_i^+ denotes the projection operator onto the space spanned by the positive energy eigenstates (electronic states) of $h_D(\boldsymbol{r})$. Because of the presence of Λ_i^+ operators, the Hamiltonian H^+ has normalizable and bound-state solutions. The $V_{ee}(\boldsymbol{r}_i,\boldsymbol{r}_j)$ in Eq. (1) denotes the electron-electron interaction. The simplest approximation of V_{ee} is given just by taking the instantaneous Coulomb interaction,

$$V_{ee}(\boldsymbol{r}_i,\boldsymbol{r}_j) = \frac{1}{r_{ij}}, \quad (3)$$

as a nonrelativistic case. In this case, the Hamiltonian (1) is usually called no-pair Dirac-Coulomb (DC) Hamiltonian (H_{DC}^+). However, the associated equation, $H_{DC}^+\Psi = E\Psi$, is not Lorentz invariant. The instantaneous Coulomb interaction operator does not contain any relativistic effect of the interaction among electrons. This is only correct to the order of α^0, where α is the fine structure constant. Therefore, the Dirac-Coulomb Hamiltonian is not appropriate for the relativistic theory, though the Hamiltonian could be a good guess for atoms and molecules composed of lighter elements in which the electron-electron interaction is expected not to be modified significantly by the introduction of the special relativity.

In QED, the relativistic effects of the electron-electron interaction are treated as a perturbation series with the fine structure constant α. The first relativistic correction to the electron-electron interaction is the Breit interaction term,[22,23] which is expressed as

$$B(\boldsymbol{r}_i,\boldsymbol{r}_j) = -\frac{1}{2r_{ij}}\left\{\boldsymbol{\alpha}_i\cdot\boldsymbol{\alpha}_j + \frac{(\boldsymbol{\alpha}_i\cdot\boldsymbol{r}_{ij})(\boldsymbol{\alpha}_j\cdot\boldsymbol{r}_{ij})}{r_{ij}^2}\right\}. \quad (4)$$

The Breit term contains the magnetic interaction introduced via the orbital and spin motions, and the retardation effect. By adding the Breit interaction term $B(\boldsymbol{r}_i,\boldsymbol{r}_j)$ to the no-pair Dirac-Coulomb Hamiltonian, we get the no-pair Dirac-Coulomb-Breit Hamiltonian, which is correct to the order of α^2.

In the present study, first-principles many-electron calculations were systematically performed for isolated $3d$ TM ions, and several $3d$ TM oxides, i.e., CoO and V_2O_3, using model clusters composed of one TM ion and coordinating six oxide ions, i.e., CoO_6^{10-} and VO_6^{9-}. The clusters were embedded in the array of point charges to take into account the external electrostatic potential. Atomic coordinates of the clusters were taken from the crystal structure data.

First, relativistic MO calculations were carried out by solving Dirac equations with the local density approximation (LDA). Four-component relativistic MOs were expressed as a linear combination of atomic orbitals. The numerically generated four-component relativistic atomic orbitals ($1s$-$4p$ for TM, and $1s$-$2p$ for O) were used as basis functions for MOs.

After the one-electron calculations of the relativistic MO, the CI calculations were carried out using Dirac-Coulomb Hamiltonian and Dirac-Coulomb-Breit Hamiltonian. Hereafter, those two approaches are simply referred to as DC and DCB, respectively. Many-electron wave functions were formed by linear combination of Slater determinants given by

$$\Psi_i = \sum_{p=1}^{M} C_{ip}\Phi_p, \quad (5)$$

where Φ_i is the ith many-electron wave function, Φ_p is the pth Slater determinant, and C_{ip} is the coefficient. In our previous TM $L_{2,3}$ XANES calculations, Slater determinants were constructed only from the MOs mainly composed of TM $2p$ and $3d$ orbitals. Sometimes O $2p$ orbitals were included. The electronic interactions to the other electrons were treated as effective potential within LDA. In the present work, all MOs were considered explicitly to construct Slater determinants. In other words, all-electron CI calculations were performed. The exchange-correlation interactions among all electrons were explicitly included. For practical calculations, the number of Slater determinants, M, was reduced. Only TM $2p$ orbitals and MOs mainly composed of TM $3d$ atomic orbitals are taken as active space. In other words, only the configurations obtained by changing the occupation in those orbitals were used to expand many-electron wave functions. Moreover, the configurations having two or more holes on TM $2p$ orbitals were not considered since they have much higher many-electron energies.

The oscillator strength of the electric dipole transition averaged over all directions is given by

$$I_{if} = \frac{2}{3}(E_f - E_i)\left|\left\langle\Psi_f\left|\sum_{k=1}^{N}\boldsymbol{r}_k\right|\Psi_i\right\rangle\right|^2, \quad (6)$$

where Ψ_i and Ψ_f are many-electron wave functions for the initial and final states, while E_i and E_f are their energies. The absolute transition energy was corrected by taking the orbital energy difference between single-electron orbitals for the Slater transition state as a reference.[6] A theoretical spectrum was made by convolving the oscillator strengths using Lorentzian functions with a full width at half maximum of 0.6 eV.

III. RESULTS AND DISCUSSION

Figure 1 shows the theoretical $L_{2,3}$ XANES of (a) Co^{2+} isolated ion and CoO, and (b) V^{3+} isolated ion and V_2O_3 obtained by DC (dashed line) and DCB approaches (solid line). It is clearly seen that in those four systems, the energy separation between L_3 and L_2 edges decreases when the Breit operators are added to the electron-electron interaction. The reduction of the energy separation between L_3 and L_2 edges due to the Breit interaction is 1.2 eV for Co^{2+} ion and CoO, and 0.7 eV for V^{3+} ion and V_2O_3. The Co L_3 edge and L_2

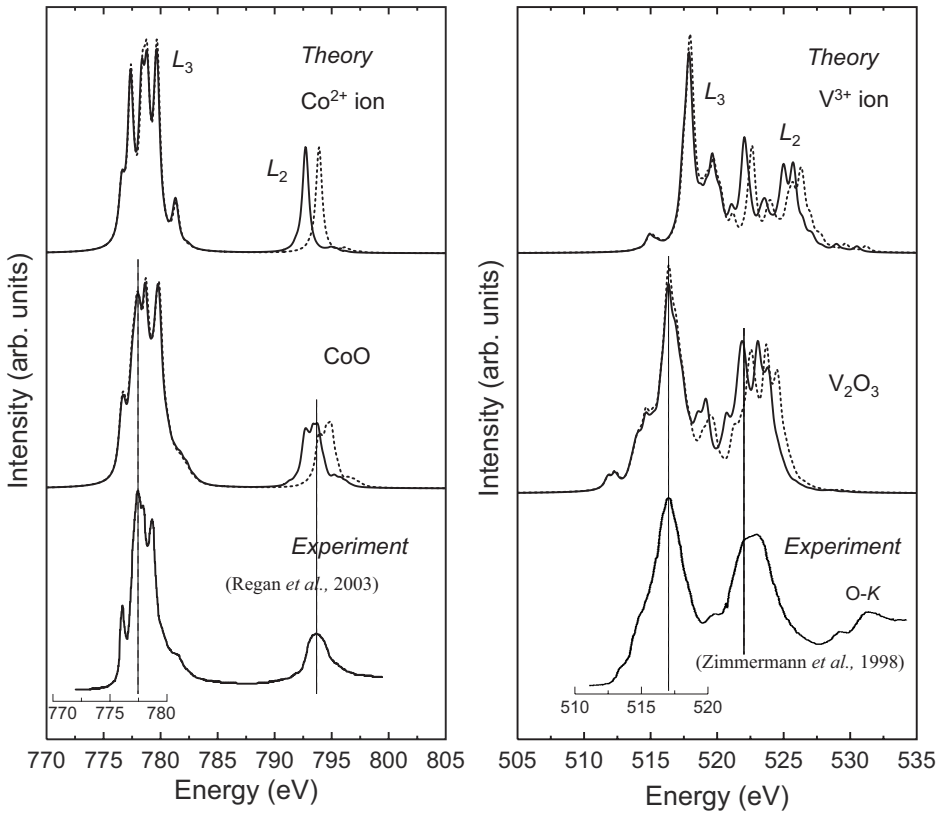

FIG. 1. Theoretical $L_{2,3}$ XANES calculated by the DC approach (dashed line) and the DCB approach (solid line) of (a) Co^{2+} ion and CoO, and (b) V^{3+} ion and V_2O_3. Experimental spectra of CoO and V_2O_3 taken from Refs. 24 and 25 and are also shown for comparison.

edge are well separated, while the V L_3 edge and L_2 edge overlap with each other (see also Figs. 2 and 3). For Co^{2+} ion and CoO, the spectral shapes are almost unchanged by the inclusion of the Breit correction term. On the contrary, for V^{3+} ion and V_2O_3, the overlap between the V L_3 edge and the V L_2 edge is enhanced by the Breit interaction, and the theoretical spectrum obtained by the DCB approach slightly differs from that obtained by the DC approach.

In Fig. 1, the experimental spectra of CoO and V_2O_3 taken from literature are also shown for comparison.[24,25] Experimental spectrum is shifted so as to align with the main peak of L_3 edge in the theoretical spectra. The theoretical spectra calculated by the DC approach overestimate the energy separation between L_3 and L_2 edges in both CoO and V_2O_3. When the DCB approach is adopted, the separation becomes smaller. In order to understand the influences of the Breit interaction term on the multiplet structures of $L_{2,3}$ XANES, the expectation values of the Breit interaction energies, E_k^{Breit}, were evaluated as

$$E_k^{\mathrm{Breit}} = \left\langle \Psi_k \left| \sum_{i=1}^{N} \sum_{j>i}^{N} B(\boldsymbol{r}_i,\boldsymbol{r}_j) \right| \Psi_k \right\rangle = \sum_{p=1}^{M} \sum_{q=1}^{M} C_{kp}^{*} C_{kq} \left\langle \Phi_p \left| \sum_{i=1}^{N} \sum_{j>i}^{N} B(\boldsymbol{r}_i,\boldsymbol{r}_j) \right| \Phi_q \right\rangle, \quad (7)$$

where Ψ_k is kth many-electron wave function obtained by the DCB approach. The expectation values of the Coulomb interaction energies, E_k^{Coulomb}, were also evaluated using a similar expression replacing $B(\boldsymbol{r}_i,\boldsymbol{r}_j)$ by $1/r_{ij}$ in Eq. (7). Table I summarizes E_i^{Coulomb} and E_i^{Breit} values for $3d$ TM ions, where i indicates the initial state (ground state) of $L_{2,3}$ XANES. As can be seen, both the Coulomb and the Breit interaction energies increase with the increase of the atomic number of TM. The Breit interaction term has a positive contribution to many-electron energies as well as the Coulomb interaction. However, the magnitude of the Breit interaction energy is about $10^{-4}(\sim\alpha^2)$ times smaller than that of the Coulomb interaction. Moreover, the Breit interaction energies are hardly affected by the valency of ions. The difference of the Breit interaction energies between the divalent and trivalent ions is at most 0.01 eV. On the contrary, the Coulomb interaction energies significantly decrease when the number of valence electrons decreases.

The Breit interaction energies were also evaluated for the final states of $L_{2,3}$ XANES. The second lower panels of Figs. 2 and 3 show the $E_f^{\mathrm{Breit}} - E_i^{\mathrm{Breit}}$ values for Co^{2+} ion, CoO, V^{3+} ion, and V_2O_3 with the transition energies, where i and f indicate the initial and final states of the TM $L_{2,3}$ XANES. The diagrams show the contribution of the Breit interaction to the transition energy for $L_{2,3}$ XANES. The expectation values of TM $2p_{1/2}$ and $2p_{3/2}$ occupation numbers ($n_{2p_{1/2}}$ and $n_{2p_{3/2}}$, respectively) at the final states of $L_{2,3}$ XANES are also plotted in the second upper panels of Figs. 2 and 3. The expectation value of the occupation number of the lth orbital at the kth many-electron eigenstate can be evaluated as

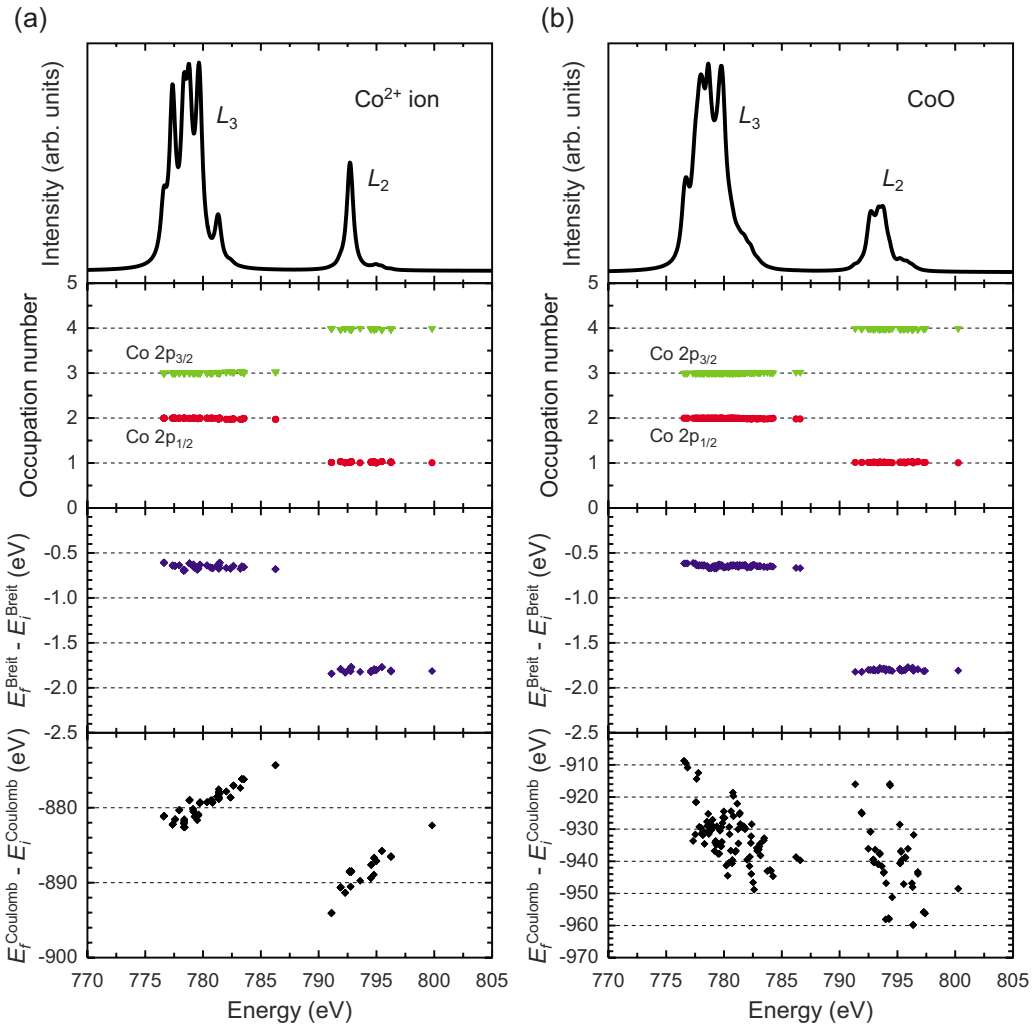

FIG. 2. (Color online) Contribution of the Breit and Coulomb interactions to the transition energies of Co $L_{2,3}$ XANES ($E_f^{\mathrm{Breit}}-E_i^{\mathrm{Breit}}$ and $E_f^{\mathrm{Coulomb}}-E_i^{\mathrm{Coulomb}}$, respectively) for (a) Co^{2+} isolated ion and (b) CoO, compared with the theoretical spectra obtained by the DCB approach. Expectation values of the occupation number of $2p_{1/2}$ and $2p_{3/2}$ orbitals at the final states of the Co $L_{2,3}$ XANES, $n_{2p_{1/2}}$ and $n_{2p_{3/2}}$, are also shown.

$$\langle \Psi_k | a_l^\dagger a_l | \Psi_k \rangle = \sum_p \sum_q C_{kp}^* C_{kq} \langle \Phi_p | a_l^\dagger a_l | \Phi_q \rangle, \qquad (8)$$

where $a_l^\dagger$ (a_l) are creation (annihilation) operators acting on the lth orbital. They are compared with theoretical spectra obtained by the DCB approach (top panels). In both Co^{2+} ion and CoO, $n_{2p_{1/2}}=2$ and $n_{2p_{3/2}}=3$ at the Co L_3 edge (775–785 eV), while $n_{2p_{1/2}}=1$ and $n_{2p_{3/2}}=4$ at the Co L_2 edge (790–800 eV). In other words, the final states at the Co L_3 edge are completely composed of $(2p_{1/2})^2(2p_{3/2})^3(3d)^{n_{3d}+1}$ configuration, while those at the Co L_2 edge are composed of $(2p_{1/2})^1(2p_{3/2})^4(3d)^{n_{3d}+1}$ configuration, where n_{3d} is the number of $3d$ electrons. The Co L_3 edge and the Co L_2 edge are well separated. On the contrary, in the V $L_{2,3}$ edge, $n_{2p_{1/2}}$ gradually decreases from 2 to 1, while $n_{2p_{3/2}}$ complementarily increases from 3 to 4 in 520–527 eV for V^{3+} ion and in 517–525 eV for V_2O_3. This means that the configuration interaction between $(2p_{1/2})^2(2p_{3/2})^3(3d)^{n_{3d}+1}$ and $(2p_{1/2})^1(2p_{3/2})^4(3d)^{n_{3d}+1}$ is large in these energy range, and the V L_3 edge and the V L_2 edge overlap with each other. As can be seen in Figs. 2 and 3, the Breit interaction has a negative contribution to the transition energies in all energy ranges (i.e., $E_f^{\mathrm{Breit}} < E_i^{\mathrm{Breit}}$), whose magnitude is about $0.2 \pm 0.1\%$ of the transition energies. This is true for the $L_{2,3}$ XANES of the other $3d$ TM ions. The magnitude of the Breit interaction energies is larger in the final states at the L_2 edge than at the L_3 edge, since the $2p_{1/2}$ electrons are bound stronger than the $2p_{3/2}$ electrons. For the Co $L_{2,3}$ XANES, $E_f^{\mathrm{Breit}}-E_i^{\mathrm{Breit}}$ is almost constant individually at L_3 and L_2 edges. They are about −0.7 eV at the L_3 edge and −1.8 eV at the L_2 edge for the Co^{2+} ion. These values are the same for CoO, though the spectral shape is significantly different from that of the Co^{2+} ion because of the existence of the crystal field. In the case of the V $L_{2,3}$ XANES, however, $E_f^{\mathrm{Breit}}-E_i^{\mathrm{Breit}}$ tends to decrease gradually from 520 to 527 eV for V^{3+} ion, and from 517 to 525 eV for V_2O_3. A large overlap between L_3 edge and L_2 edge can be seen in these cases.

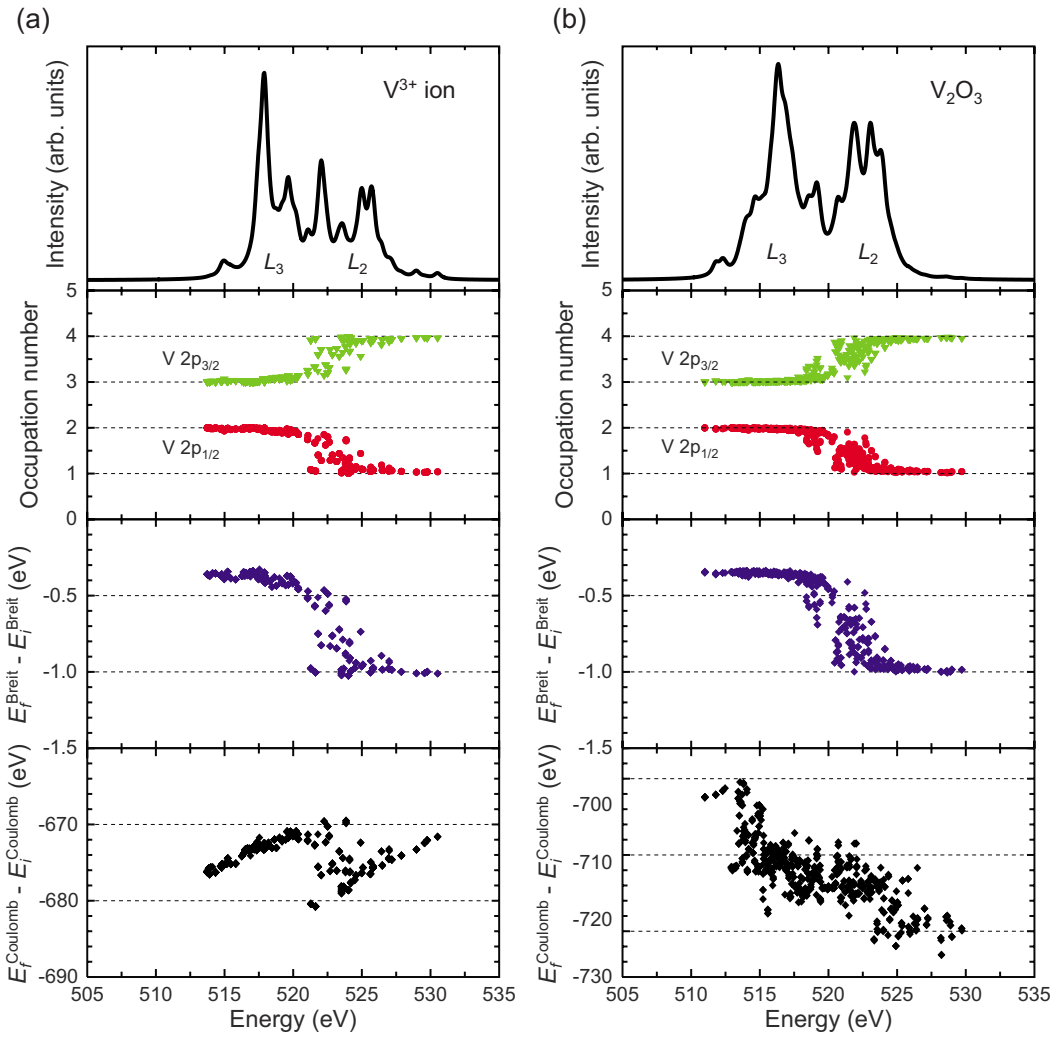

FIG. 3. (Color online) Same as Fig. 2, but for (a) V^{3+} ion and (b) V_2O_3.

TABLE I. Coulomb and Breit interaction energies ($E_i^{Coulomb}$ and E_i^{Breit}) at the initial states of the $L_{2,3}$ XANES for divalent and trivalent 3*d* TM ions obtained by the DCB approach.

Ion	$E_i^{Coulomb}$ (eV)	E_i^{Breit} (eV)
Sc^{3+} (d^0)	7065.34	2.70
Ti^{2+} (d^2)	8283.03	3.23
Ti^{3+} (d^1)	7946.67	3.24
V^{2+} (d^3)	9267.68	3.83
V^{3+} (d^2)	8904.67	3.83
Cr^{2+} (d^4)	10334.82	4.49
Cr^{3+} (d^3)	9944.75	4.50
Mn^{2+} (d^5)	11487.83	5.22
Fe^{2+} (d^6)	12739.21	6.06
Co^{2+} (d^7)	14085.21	6.99
Ni^{2+} (d^8)	15530.55	8.01
Cu^{2+} (d^9)	17078.51	9.12

The behavior of the Coulomb interaction energies is quite different from the Breit interaction energies. The lower panels in Figs. 2 and 3 show the contribution of the Coulomb interaction to the transition energy for the $L_{2,3}$ XANES. In every four systems, $E_f^{Coulomb} - E_i^{Coulomb}$ varies considerably among the final states. By comparing Co^{2+} and CoO (V^{3+} and V_2O_3), the distributions of $E_f^{Coulomb} - E_i^{Coulomb}$ are significantly different. They are strongly affected by the ligand field.

From Figs. 2 and 3, a good correlation can be found between $E_f^{Breit} - E_i^{Breit}$ and $n_{2p_{3/2}}$ ($n_{2p_{1/2}}$). As $n_{2p_{3/2}}$ increases ($n_{2p_{1/2}}$ decreases), $E_f^{Breit} - E_i^{Breit}$ decreases. Figure 4 visualizes the relationship between $n_{2p_{3/2}}$ and $E_f^{Breit} - E_i^{Breit}$ for Co^{2+} and V^{3+} ions. The straight lines in Fig. 4 are the results of the least-square fits. $E_f^{Breit} - E_i^{Breit}$ is linearly dependent on $n_{2p_{3/2}}$ (or $n_{2p_{1/2}}$). This means the nondiagonal matrix elements of the Breit interaction operators, $\langle \Phi_p | \Sigma_{i,j} B(\boldsymbol{r}_i, \boldsymbol{r}_j) | \Phi_q \rangle (p \neq q)$, are so small that they can hardly contribute to the multiplet energies. In other words, the Breit "correlation" effects among TM 2*p* and 3*d* electrons are negligibly small in the case of the 3*d* TM $L_{2,3}$ XANES. The diagonal matrix elements, $\langle \Phi_p | \Sigma_{i,j} B(\boldsymbol{r}_i, \boldsymbol{r}_j) | \Phi_p \rangle$, just make a shift of the eigenval-

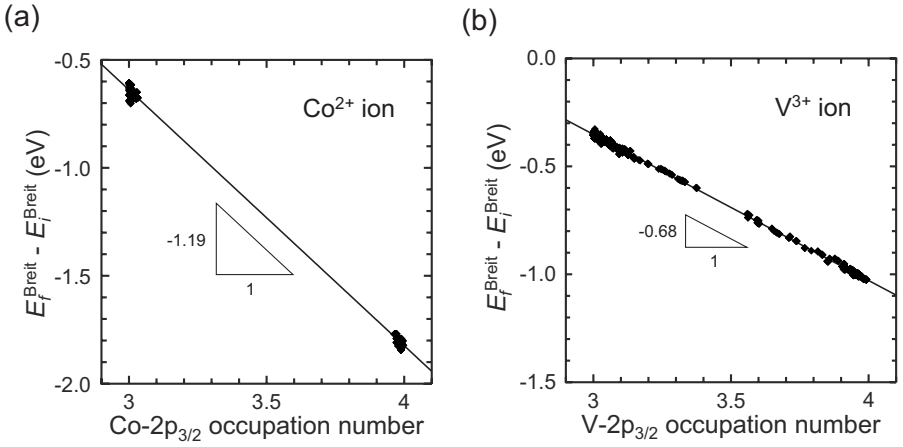

FIG. 4. $E_f^{\mathrm{Breit}}-E_i^{\mathrm{Breit}}$ at the final states corresponds to the $L_{2,3}$ XANES of (a) Co^{2+} and (b) V^{3+} ions as a function of the TM $2p_{3/2}$ occupation number ($n_{2p_{3/2}}$). The straight lines are results of the least-square fits.

ues of the Hamiltonian matrix, and the magnitude of the energy shift only depends on whether the $2p$ core-hole is located on the $2p_{1/2}$ or $2p_{3/2}$. The gradients of the straight lines in Fig. 4 indicate the difference of the shift of the multiplet energies due to the Breit interaction between $(2p_{1/2})^2(2p_{3/2})^3(3d)^{n_{3d}+1}$ configuration ($n_{2p_{3/2}}=3$) and $(2p_{1/2})^1(2p_{3/2})^4(3d)^{n_{3d}+1}$ configuration ($n_{2p_{3/2}}=4$). These values are −1.19 and −0.68 eV for the Co $L_{2,3}$ and the V $L_{2,3}$ XANES, respectively, which correspond to the reduction of the L_3-L_2 energy separation due to the Breit interaction as shown in Fig. 1.

The difference of the energy shift between two configurations due to the Breit interaction is also evaluated for the other $3d$ TM ions. Results are summarized in Table II. The reduction of the L_3-L_2 energy separation becomes larger when the atomic number of the $3d$ TM ion increases, since the $2p$ electrons are more strongly bound and the spin-orbit splitting between $2p_{3/2}$ and $2p_{1/2}$ becomes larger. They are independent of the valency of the ion and the existence of the ligand field (not shown in Table II), which can be ascribed to the small Breit correlation effects among core $2p$ and valence $3d$ electrons. Therefore, in the case of $3d$ TM $L_{2,3}$ XANES, the main contributions of the Breit interaction can be taken into account by reducing the relative energy difference between the multiplet for $(2p_{1/2})^2(2p_{3/2})^3(3d)^{n_{3d}+1}$ and $(2p_{1/2})^1(2p_{3/2})^4(3d)^{n_{3d}+1}$ configurations. The amount of reduction is element specific and may easily be included into the effective spin-orbit coupling constants of TM $2p$ orbitals.

Note that the above discussion is valid only for $3d$ TM elements or lighter ones. For heavier elements, the Breit correlation effects become larger and may change the multiplet structures. Furthermore, the higher order correction of electron-electron interaction should also affect the transition energy of $L_{2,3}$ XANES. Currently, calculations including higher order perturbations are prohibitively expensive even in the case of isolated atoms using the present computational scheme.

IV. CONCLUSIONS

All-electron relativistic CI calculations of the $L_{2,3}$ XANES for $3d$ TM ions and their oxides have been made based on the no-pair Dirac-Coulomb and Dirac-Coulomb-Breit Hamiltonians. The effects of the Breit interaction term on the $3d$ TM $L_{2,3}$ XANES spectra have been discussed. The major results of this paper can be summarized as follows:

(1) TM $L_{2,3}$ XANES of Co^{2+} ion, CoO, V^{3+} ion, and V_2O_3 have been calculated. In those four systems, the energy separation between L_3 and L_2 edges decreases when the Breit interaction term is added to the electron-electron interaction.

(2) The theoretical spectra of CoO and V_2O_3 obtained by the DC approach overestimate the energy separation between L_3 and L_2 edges of the experimental spectra.

(3) The Breit interaction term has positive contributions to the many-electron eigenvalues as well as the Coulomb interaction. The Breit interaction energy is 4 orders of magnitude smaller than the Coulomb interaction energy.

(4) The contributions of the Breit interaction term to the transition energies of $3d$ TM $L_{2,3}$ XANES, $E_f^{\mathrm{Breit}}-E_i^{\mathrm{Breit}}$, are negative, whose magnitude is about $0.2\pm0.1\%$ of the transition energies. $E_f^{\mathrm{Breit}}-E_i^{\mathrm{Breit}}$ is almost constant individually at L_3 and L_2 edges, except for those in the energy region where

TABLE II. Relative shift of multiplet energies due to the Breit interaction between $(2p_{1/2})^2(2p_{3/2})^3(3d)^{n_{3d}+1}$ and $(2p_{1/2})^1(2p_{3/2})^4(3d)^{n_{3d}+1}$ configurations for isolated $3d$ TM ions. Figure 4 shows how to obtain these values.

Valency	Sc	Ti	V	Cr	Mn	Fe	Co	Ni	Cu
2+		−0.58	−0.68	−0.78	−0.91	−1.04	−1.19	−1.34	−1.52
3+	−0.49	−0.58	−0.68	−0.78					

overlaps between L_3 edge and L_2 edge are evident. They are independent of the valency of the TM or the crystal field, while the contributions of the Coulomb interaction to the transition energy, $E_f^{\text{Coulomb}} - E_i^{\text{Coulomb}}$, strongly depend on the crystal field.

(5) $E_f^{\text{Breit}} - E_i^{\text{Breit}}$ is linearly dependent on $n_{2p_{3/2}}$ ($n_{2p_{1/2}}$) at the final states of the $3d$ TM $L_{2,3}$ XANES. The result clearly implies that the Breit correlation effects are negligibly small, and the diagonal matrix elements just make a shift of the many-electron eigenvalues.

(6) In the case of the $3d$ TM $L_{2,3}$ XANES, the main contributions of the Breit interactions in the $L_{2,3}$ XANES can be taken into account just by reducing the relative energy difference between the multiplet for $(2p_{1/2})^2(2p_{3/2})^3(3d)^{n_{3d}+1}$ and $(2p_{1/2})^1(2p_{3/2})^4(3d)^{n_{3d}+1}$ configurations. The amount of reduction is element specific.

ACKNOWLEDGMENTS

This work was supported by three programs from the Ministry of Education, Culture, Sports, Science and Technology of Japan, i.e., the Grant-in-Aids for Scientific Research (A), Priority Area on atomic scale modification (No. 474), and the global COE program.

*ikeno@t02.mbox.media.kyoto-u.ac.jp

[1] I. Tanaka, T. Mizoguchi, and T. Yamamoto, J. Am. Ceram. Soc. **88**, 2013 (2005).
[2] T. Mizoguchi, I. Tanaka, S. Yoshioka, M. Kunisu, T. Yamamoto, and W. Y. Ching, Phys. Rev. B **70**, 045103 (2004).
[3] F. de Groot, Coord. Chem. Rev. **249**, 31 (2005).
[4] F. M. F. de Groot, J. Electron Spectrosc. Relat. Phenom. **67**, 529 (1994).
[5] A. Kotani, J. Electron Spectrosc. Relat. Phenom. **100**, 75 (1999).
[6] K. Ogasawara, T. Iwata, Y. Koyama, T. Ishii, I. Tanaka, and H. Adachi, Phys. Rev. B **64**, 115413 (2001).
[7] H. Ikeno, I. Tanaka, Y. Koyama, T. Mizoguchi, and K. Ogasawara, Phys. Rev. B **72**, 075123 (2005).
[8] H. Ikeno, T. Mizoguchi, Y. Koyama, Y. Kumagai, and I. Tanaka, Ultramicroscopy **106**, 970 (2006).
[9] J. B. Mann and W. R. Johnson, Phys. Rev. A **4**, 41 (1971).
[10] M. H. Chen, B. Crasemann, and H. Mark, Phys. Rev. A **25**, 391 (1982).
[11] M. H. Chen, K. T. Cheng, and W. R. Johnson, Phys. Rev. A **47**, 3692 (1993).
[12] K. T. Cheng and M. H. Chen, Phys. Rev. A **53**, 2206 (1996).
[13] Y. Ishikawa and H. M. Quiney, Phys. Rev. A **47**, 1732 (1993).
[14] Y. Ishikawa and K. Koc, Phys. Rev. A **50**, 4733 (1994).
[15] E. Eliav, U. Kaldor, and Y. Ishikawa, Phys. Rev. A **49**, 1724 (1994).
[16] E. Eliav, U. Kaldor, and Y. Ishikawa, Phys. Rev. A **51**, 225 (1995).
[17] P. Indelicato, S. Boucard, and E. Lindroth, Eur. Phys. J. D **3**, 29 (1998).
[18] A. M. Costa, M. C. Martins, J. P. Santos, P. Indelicato, and F. Parente, J. Phys. B **39**, 2355 (2006).
[19] R. D. Deslattes, E. G. Kessler, Jr., P. Indelicato, L. de Billy, E. Lindroth, and J. Anton, Rev. Mod. Phys. **75**, 35 (2003).
[20] J. Sucher, Phys. Rev. A **22**, 348 (1980).
[21] M. H. Mittleman, Phys. Rev. A **24**, 1167 (1981).
[22] G. Breit, Phys. Rev. **34**, 375 (1929).
[23] G. Breit, Phys. Rev. **39**, 616 (1932).
[24] T. J. Regan, H. Ohldag, C. Stamm, F. Nolting, J. Lüning, J. Stöhr, and R. L. White, Phys. Rev. B **64**, 214422 (2001).
[25] R. Zimmermann, R. Claessen, F. Reinert, P. Steiner, and S. Hüfner, J. Phys.: Condens. Matter **10**, 5697 (1998).